

# Supplementary Material: Explosive synchronization in adaptive and multilayer networks

Xiyun Zhang,<sup>1</sup> Stefano Boccaletti,<sup>2,3,\*</sup> Shuguang Guan,<sup>1</sup> and Zonghua Liu<sup>1,†</sup>

<sup>1</sup>Department of Physics, East China Normal University, Shanghai, 200062, China

<sup>2</sup>CNR- Institute of Complex Systems, Via Madonna del Piano 10, 50019 Sesto Fiorentino, Florence, Italy

<sup>3</sup>The Italian Embassy in Israel, 25 Hamered Street, 68125 Tel Aviv, Israel

(Dated: December 29, 2014)

PACS numbers:

We here discuss the issue of the absence of correlation features associated with the behavior reported in Figures 1 and 2 of the main text.

The fraction  $1 - f$  of oscillators in the network(s) is not affected by the adaptation mechanism and is, by definition and construction, not displaying *any form* of correlation between nodes' frequencies and coupling strength. As for the fraction  $f$  of nodes which are, instead, affected by the adaptation rule, it is determinant to notice that the local order parameters defined in the text are *fully independent* on the actual instantaneous phase of the considered oscillators (they, indeed, depend *only and solely* on the degree of synchronization of the neighboring oscillators of each of these nodes).

And, indeed, Fig. 1 show that *no correlation features at all* between the oscillators' frequencies and their coupling

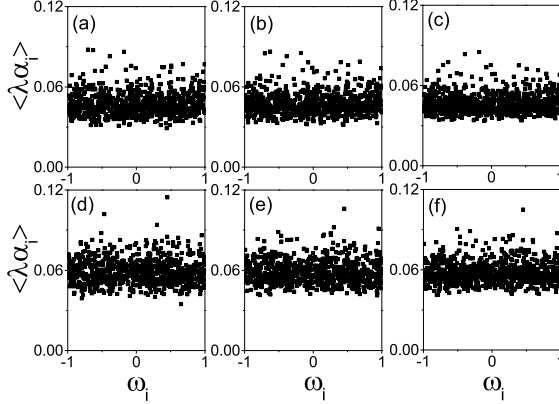


FIG. 1: Correlation properties just before the forward transition to synchronization. Panels (a),(b) and (c) refer to the single network case, i.e. to the scenario reported in Fig. 1 of the main text. They corresponds to  $f = 0.8$ ,  $\lambda = 0.16$  (i.e. at the forward transition point to synchronization), a single Erdős-Rényi network with 1,000 nodes,  $\langle k \rangle = 12$ , and a uniform frequency distribution in the range  $[-1; 1]$ . Vertical axes report the values of  $\langle \lambda \alpha_i \rangle$ , i.e. the time averages of  $\lambda \alpha_i$  over 5,000 (a), 10,000 (b) and 50,000 (c) time steps. Panels (d),(e) and (f) account, instead, for the two-layer case, with  $N = 1,000$ ,  $f = 0.8$ ,  $\lambda = 0.2$  (once again at the forward transition point), and all other parameters as in the caption of Fig. 2 (a) of the main text. Vertical axes report the values of  $\langle \lambda \alpha_i \rangle$ , i.e. the time averages of  $\lambda \alpha_i$  over 5,000 (d), 10,000 (e) and 50,000 (f) time steps. Exactly the same qualitative scenario (not shown) occurs for the nodes in layer II.

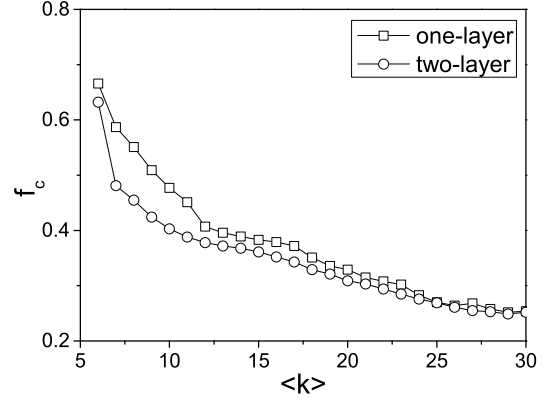


FIG. 2: Dependency of the critical fraction  $f_c$  on the system parameter  $\langle k \rangle$  where the results are obtained by taking average on 10 realizations. The curve with “squares” represents the case of a single network of Fig. 1 in the main text where the average degree  $\langle k \rangle$  change from 6 to 30. While the curve with “circles” denotes the case of two-layered network of Fig. 2(a) in the main text, where the two layers have both the same size  $N$  and the same average  $\langle k \rangle$ .

strengths are associated (at the onset of explosive synchronization in both single-layer and two-layers networks) neither in their short-, nor in their intermediate-, nor even in their long-time averages (as compared with all other relevant involved time scales).

To check the dependency of the critical fraction  $f_c$  on the system parameter  $\langle k \rangle$ , we first focus on the single network of Fig. 1 in the main text. Instead of the fixed average degree  $\langle k \rangle = 12$ , we here let  $\langle k \rangle$  change from 6 to 30. We find, numerically, that  $f_c$  decreases monotonously with the increase of  $\langle k \rangle$ . The “squares” in Fig. 2 shows the result. Then, we move to the case of the two-layered network. We take the network of Fig. 2(a) in the main text as an example. We let the two layers have both the same size  $N$  and the same average  $\langle k \rangle$  but let  $\langle k \rangle$  change from 6 to 30. Very interestingly, we observe the similar decreasing phenomenon, see the “circles” in Fig. 2, indicating that denser connections make ES occur earlier.

Fig. 3 reports the solutions of Eqs. (6) and (7) in the main text. In both cases (illustrated by panel (a) and (b) of the Figure), it is easy to notice the presence of an unstable middle branch, which is responsible for the hysteretic loop associated

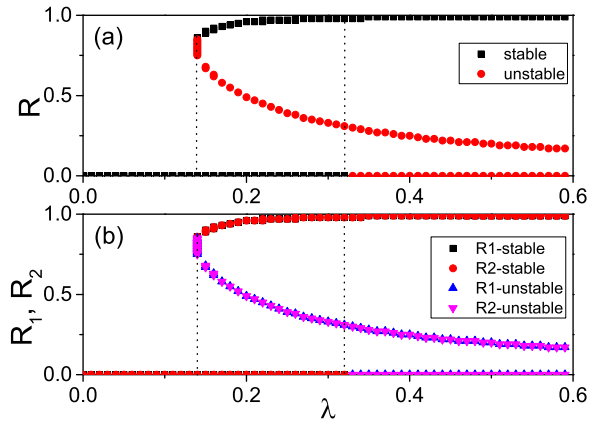


FIG. 3: (color online). Analytical solutions for the order parameter  $R$ . (a)  $R$  vs.  $\lambda$  for the single ER network of Eq. (1) with  $f = 1$  in the main text.  $R$  is here calculated from Eq. (6) in the main text, and parameters are the same as those in Fig. 1 (b)  $R$  vs.  $\lambda$  in the main text for the two-layered ER network of Eqs. (2) with  $f = 1$  in the main text.  $R_1$  (“squares” and “up triangles”) and  $R_2$  (“circles” and “down triangles”) are evaluated from Eq. (7) in the main text and the parameters are the same as in Fig. 2(a) in the main text. In all cases, “dotted lines” are just guides for the eye.

to ES, and observed in Figs. 1 and 2 in the main text.

\* Electronic address: stefano.boccaletti@gmail.com

† Electronic address: zhliu@phy.ecnu.edu.cn